

Human spermbots for patient-representative 3D ovarian cancer cell treatment

Haifeng Xu^{†1}, Mariana Medina-Sánchez^{*†}, Wunan Zhang,[†] Melanie Seaton[§], Daniel R. Brison^{Ψ,ζ}, Richard J. Edmondson^{Δ,Ω}, Stephen S. Taylor[§], Louisa Nelson[§], Kang Zeng^π, Steven Bagley^π, Carla Ribeiro^α, Lina P. Restrepo^α, Elkin Lucena^α, Christine K. Schmidt^{*,§}, Oliver G. Schmidt^{*†1‡2}

[†] Institute for Integrative Nanosciences, Leibniz IFW Dresden, Helmholtzstraße 20, 01069 Dresden, Germany

¹ School of Science, TU Dresden, 01062 Dresden, Germany

^Ψ Maternal and Fetal Health Research Centre, Division of Developmental Biology and Medicine, School of Medical Sciences, Faculty of Biology, Medicine and Health, University of Manchester, Manchester Academic Health Sciences Centre, St. Mary's Hospital, Manchester, M13 9WL, United Kingdom

^ζ Department of Reproductive Medicine, St. Mary's Hospital, Manchester University NHS Foundation Trust, Manchester Academic Health Sciences Centre, Manchester, M13 9WL, United Kingdom

^Δ Gynaecological Oncology, Division of Cancer Sciences, School of Medical Sciences, Faculty of Biology, Medicine and Health, Manchester Academic Health Science Centre, University of Manchester, Manchester, United Kingdom

^Ω St Mary's Hospital, Central Manchester NHS Foundation Trust, Manchester Academic Health Science Centre, Level 5, Research Floor, Oxford Road, Manchester M13 9WL, United Kingdom

^α Colombian Center of Fertility and Sterility (CECOLFES), Bogotá, Colombia

[§] Manchester Cancer Research Centre, Division of Cancer Sciences, School of Medical Sciences, Faculty of Biology, Medicine and Health, University of Manchester, 555 Wilmslow Road, Manchester, M20 4GJ, United Kingdom

^π Advanced Imaging and Flow Cytometry, Cancer Research UK Manchester Institute, University of Manchester, Alderley Park, SK10 4TG, United Kingdom

[‡] Material Systems for Nanoelectronics, TU Chemnitz, Reichenhainer Straße 70, 09126 Chemnitz, Germany

² Research Center for Materials, Architectures and Integration of Nanomembranes (MAIN), Rosenbergstraße 6, TU Chemnitz, 09126 Chemnitz, Germany

Supplementary Figures

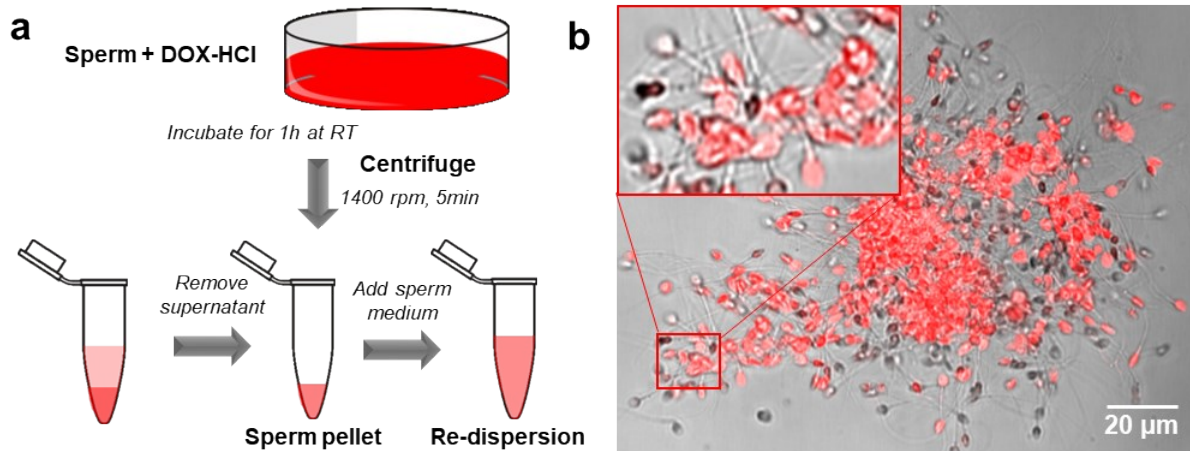


Figure S1. DOX-HCl loading of human sperm. (a) Experimental pipeline for loading sperm cells with DOX-HCl. RT: room temperature. (b) Merged fluorescence and bright-field images of DOX-HCl-loaded sperm. Red color indicates autofluorescence of DOX-HCl. DOX-HCl: doxorubicin hydrochloride.

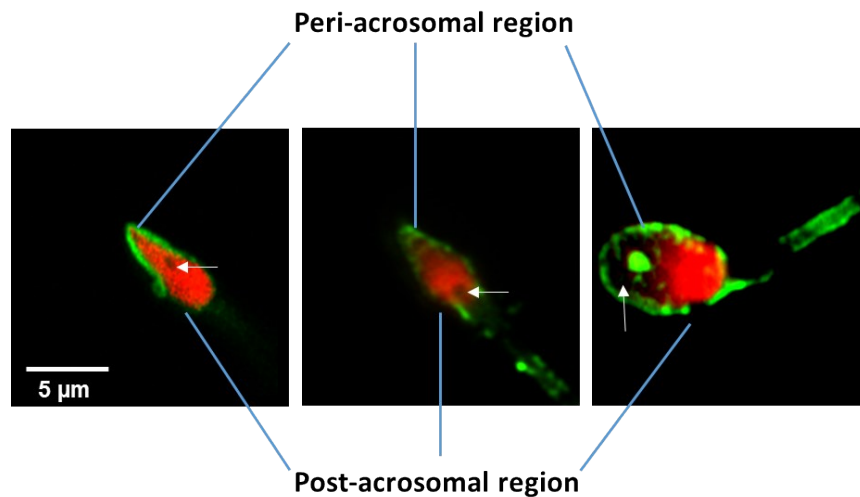
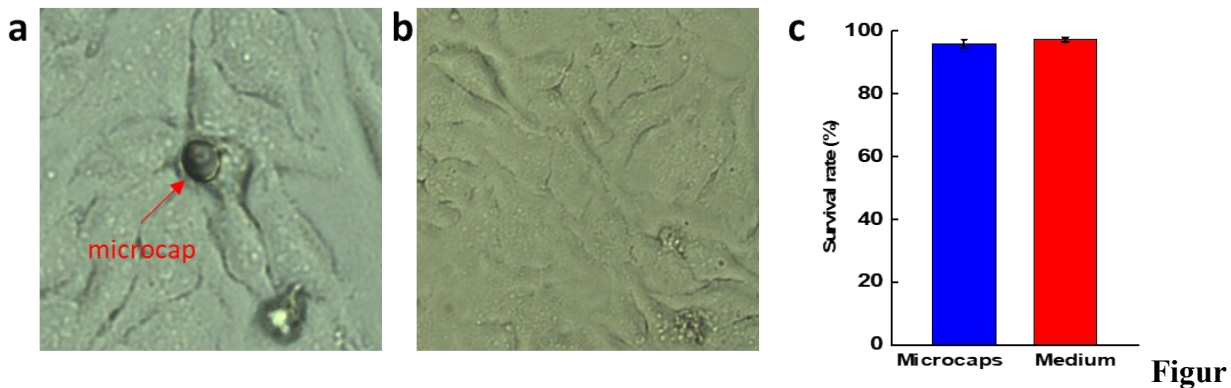


Figure S2. DOX-HCl localizes to the nucleus inside the sperm head. Detailed information on three different sperm cells. White arrows point at structures resembling nuclear vacuoles. DOX-HCl autofluorescence shown in red; Alexa Fluor 488-conjugated wheat germ agglutinin (AF488-WGA) shown in green. DOX-HCl: doxorubicin hydrochloride.



e S3. Biocompatibility evaluation of microcaps used in this study. Optical images of (a) microcap-treated group and (b) cell medium control group. (c) HeLa cell survival after 3 days of cell culture. Data represent means of n=4 replicates +/- standard deviations.

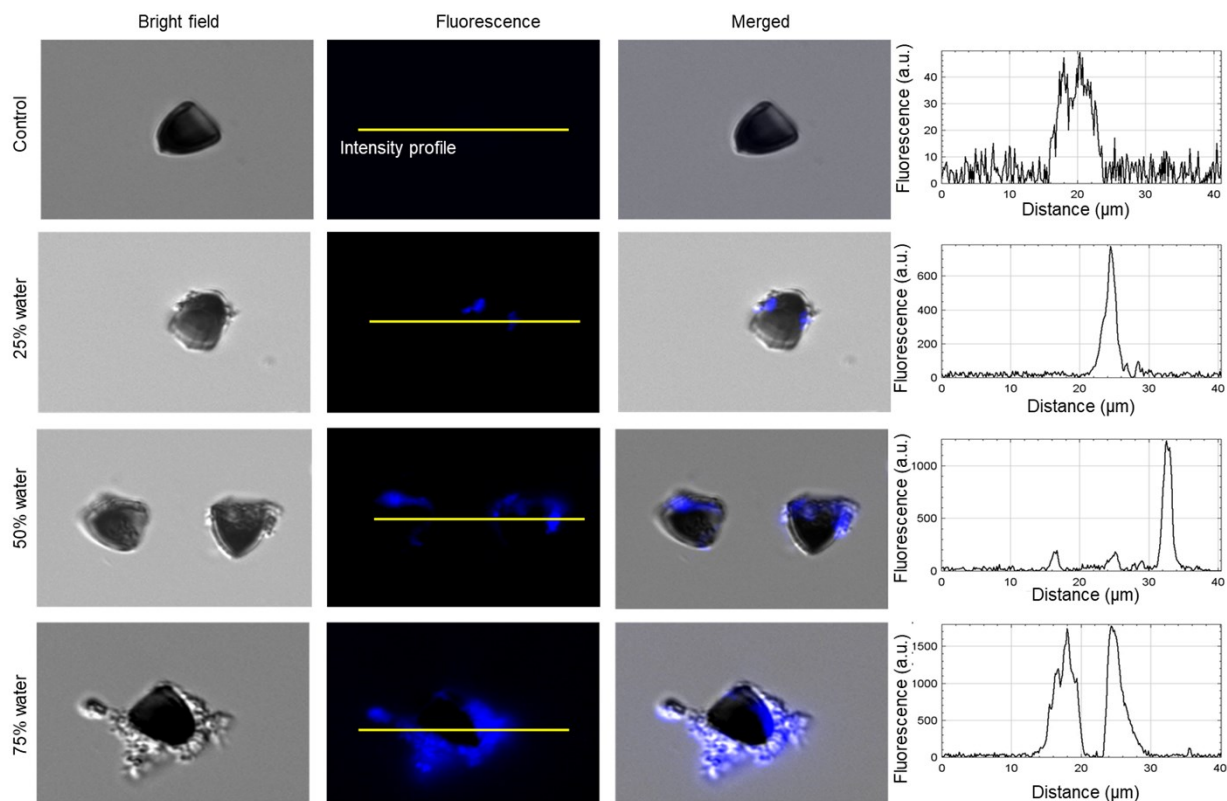


Figure S4. Camptothecin (CPT) loading onto streamlined sperm caps. (a) Fluorescence images of microcaps loaded with CPT prepared with different precipitation reagents (excitation =

350 nm; emission = 435 nm). (b) Emission curve of CPT (excitation = 350 nm). (c) Averaged CPT loading capacity of single microcaps. Data represent means of n=3 replicates +/- standard deviations.

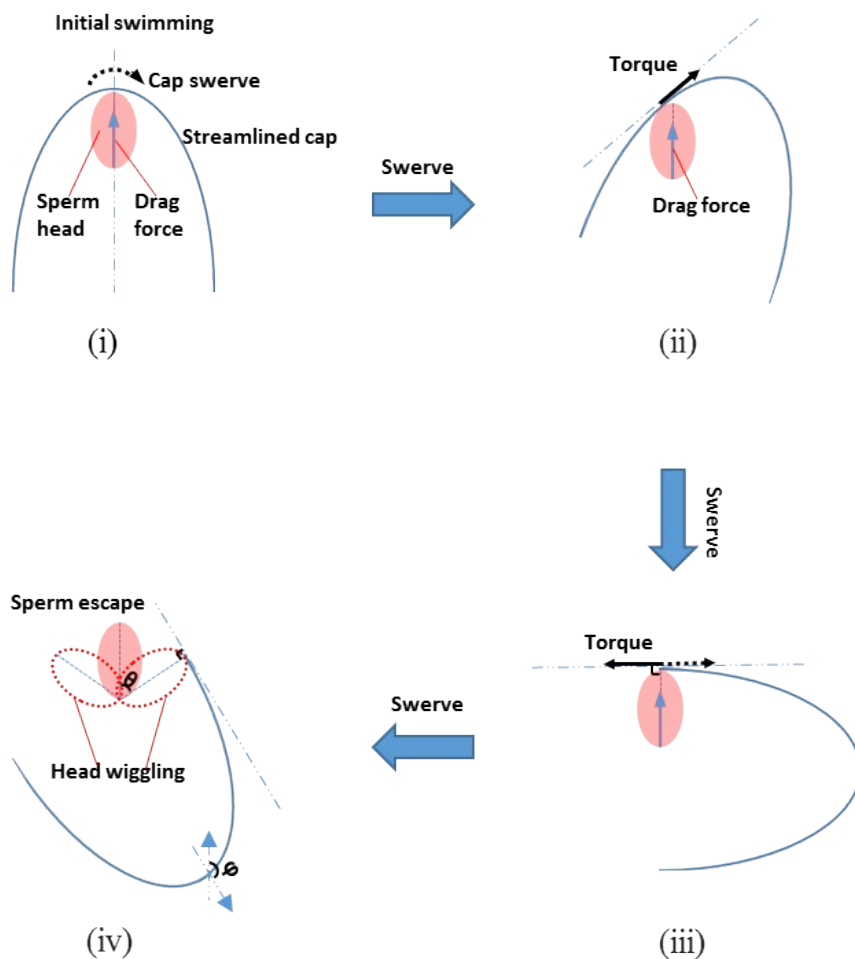


Figure S5. Ejection mechanism of sperm from streamlined caps. The sperm head was regarded as an ellipse in its projective plane, in which the projection of the streamlined cap takes the shape of a semi-ellipsoid structure (blue line). The encapsulated sperm bears a drag force along its long axis (i) and can only move tangentially in the semi-ellipsoid structure of the cap. The cap swerving is carried out by rapidly changing the direction of the imposed magnetic field. In this situation the torque is always directed along the tangential line in the same direction of the

drag force during continuous swerving of the cap (ii). Sperm escape occurs when the drag force becomes perpendicular to the torque/tangential line (iii). After taking the wiggling angle of the sperm head (θ , 57° , middle panel) into account, the resultant critical decoupling angle is shown as ϕ (147° , iv).

Video S1. 3D construction of a DOX-HCl-loaded human sperm stained with Alexa Fluor 488-conjugated wheat germ agglutinin (AF488-WGA).

Video S2. 3D construction showing a DOX-HCl-loaded sperm head that has penetrated into an ovarian cancer OCM.66-1 cell.

Video S3. Coupling of a human sperm to a streamlined cap.

Video S4. Guidance of a streamlined spermbot propelled by 3 human sperm.

Video S5. Guidance of 5 human spermbots.

Video S6. Coupling, transport and release of a spermbot toward a HeLa cancer cell spheroid.